

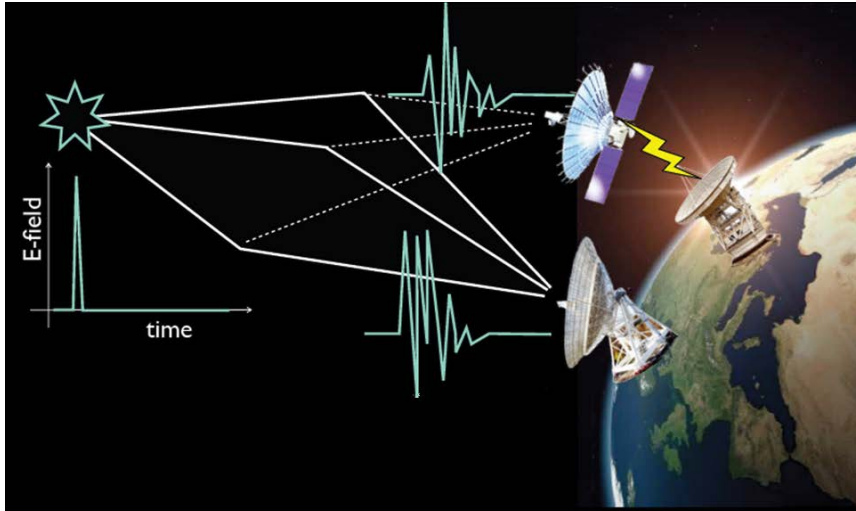
Probing of interstellar plasma distribution in the direction to pulsars PSR 0525+21 and 1919+21 with RadioAstron mission

A.S. Andrianov, T. V. Smirnova, V. I. Shishov, M. V. Popov,
C. Gwinn

Overview

- The RadioAstron spacecraft presents a unique opportunity to measure properties of interstellar scattering.
- The fluctuations responsible for scattering radio waves from astronomical sources are small-scale (~ 0.1 AU) fluctuations in the electron density of the interstellar medium.
- There are three main components of interstellar plasma inhomogeneities – A (galactic scale ~ 10 kpc), B (50-300 pc), C (10 pc) components.
- Scattering of nearby pulsars and intra-day variable quasars point to the existence of a component of the interstellar medium (B,C) which has properties quite different from the more distant, diffuse ISM (A).
- We observed several nearby pulsars as part of RadioAstron's Science Program. We present here results concerning the distribution and properties of scattering material in the direction to pulsar B1919+21 and pulsar B0525+21.

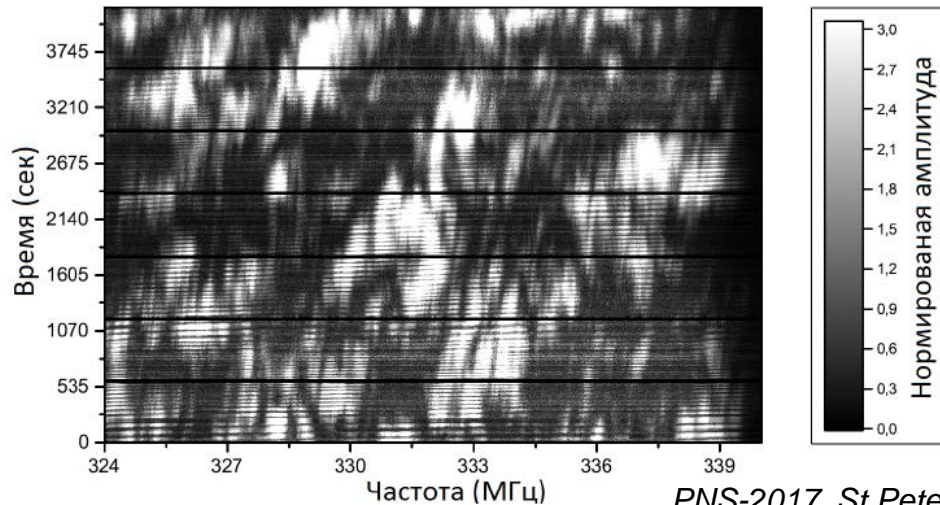
Interstellar scintillation



- The scattering causes angular broadening, pulse broadening, intensity modulation, or scintillation, and distortion of radio spectra. Scattering convolves a signal emitted at the source with an impulse-response function, reflecting reinforcement or cancellation of radiation from along different paths, with different lengths.
- Relative lengths of the different paths change with observer position, so that the impulse-response function changes with position. For most sources and wavelengths of interest, the lateral scale of that change is greater than the diameter of the Earth; however, in many interesting cases it is smaller than the distance between Earth and the radio telescope aboard the Spektr-R spacecraft in high Earth orbit. Thus, only RadioAstron, in concert with ground antennas, can simultaneously observe the impulse-response function in two locations.

$$E(\vec{\rho}, f, t) = u(\vec{\rho}, f, t) h(f, t)$$

PSR B1919+21



$$t_{dif} = \frac{\rho}{V_{\perp}}, \rho = \frac{1}{k\theta_{scat}}; f_{dif} = \frac{c}{\pi Z\theta_{scat}^2}$$

RadioAstron



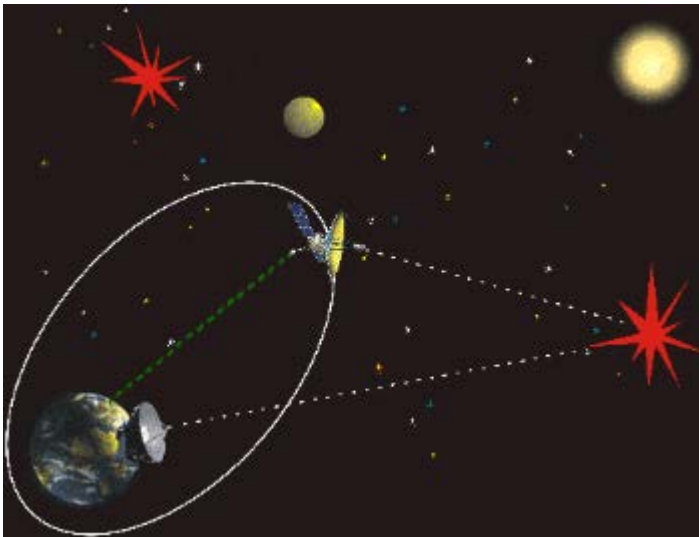
- RadioAstron – space-ground interferometer with maximum baseline projection up to 350 000 km
- Frequency bands:

P(327МГц)

L (1668 МГц)

C (4828 МГц)

K (22 ГГц)



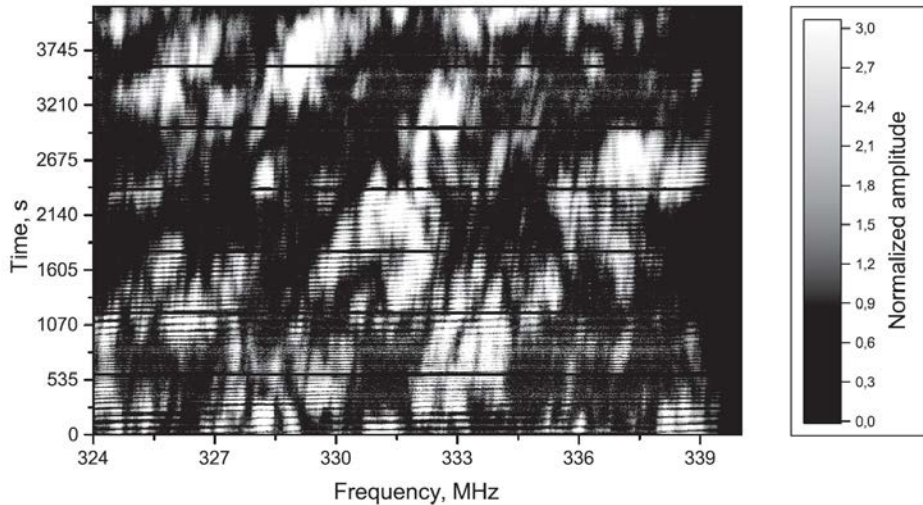
- Launched 18 July 2011 г.

Observations of PSR B1919+21

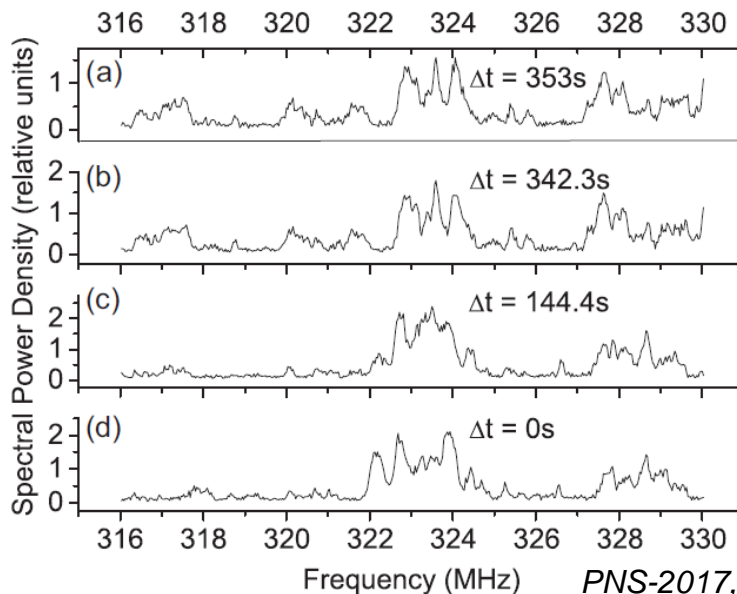
- 04.07.2012, Projection of base is 60 000 km
- Frequency 316 MHz, Bandwidth is 16 MHz
- Time duration is 69.5 min
- Telescopes: RA, Green Bank, Westerbork
- $DM = 12.43$, $Z = 1$ kpc, $P_1 = 1.337$ s, ($b = 3.5^\circ$, $l = 55.8^\circ$)

- Data were recorded in 570 s scans with 30 s gaps between scans. On-pulse window includes intensities inside of mean profile on its 0.1 amplitude level (40 ms). The off-pulse window was offset from the pulse by half of period.
- Correlator ASC FIAN for getting complex cross-spectra.
- Time resolution $\Delta t = 1.34$ s $\Delta f = 31.25$ kHz (512 channels)

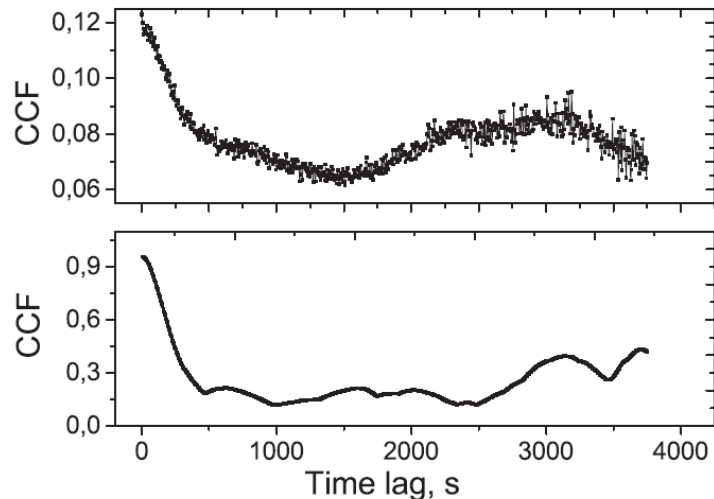
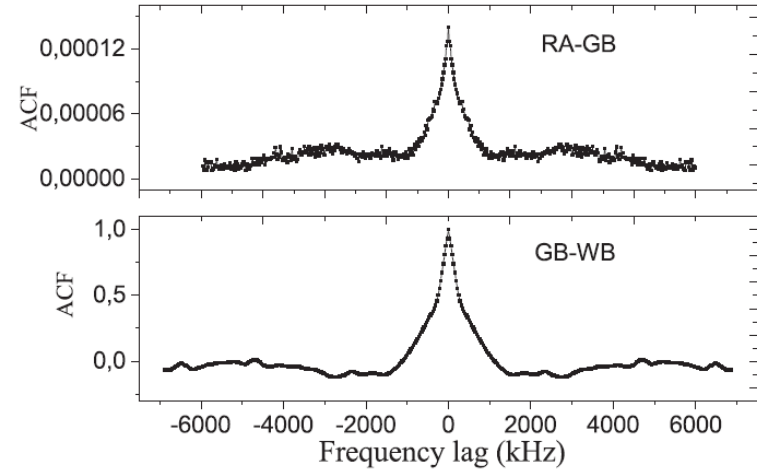
PSR B1919+21



- Individual pulses show two frequency scales: narrow (400 KHz) and wide (1500 KHz)
- Slope in dynamic spectra due to refraction on cosmic prism
- Modulation index $m \sim 0.7 - 1.0$ on time scale ~ 500 sec.
- Strong scattering in direction to PSR B1919+21.



1919+21 CCF



- Coherence function on ground baseline:

$$J_2(\vec{b}, \Delta f) = \langle |I(\vec{\rho}, \vec{\rho} + \vec{b}, f, t) I^*(\vec{\rho}, \vec{\rho} + \vec{b}, f + \Delta f, t)| \rangle$$

- Space-ground baseline:

$$J_1(\vec{b}, \Delta f) = \langle |I(\vec{\rho}, \vec{\rho} + \vec{b}, f, t) I^*(\vec{\rho}, \vec{\rho} + \vec{b}, f + \Delta f, t)| \rangle$$

- Break in CCF on GB-WB baseline shows on two-scales structure.
- No break on RA-GB indicates the absence of wide-scale structure on a large baseline
- From CCF we determine frequency and time scales:

$$\Delta f_{dif} = 330 \text{ kHz} \quad \text{и} \quad \Delta f_{wide} = 700 \text{ kHz} \quad \Delta t_{dif} = 290 \text{ s}$$

- In the regime of strong scintillation:

$$J_1(\vec{b}, \Delta f) = |B_u(f)|^2 + |B_u(\vec{b})|^2.$$

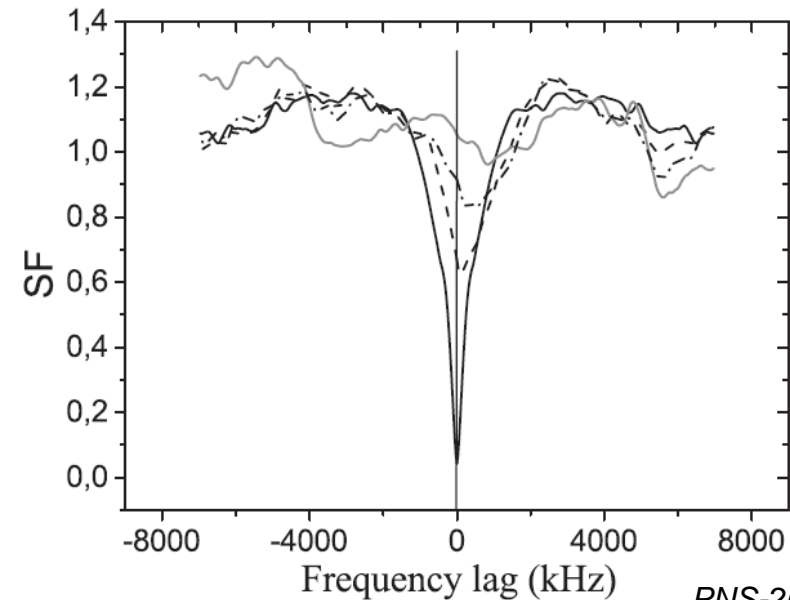
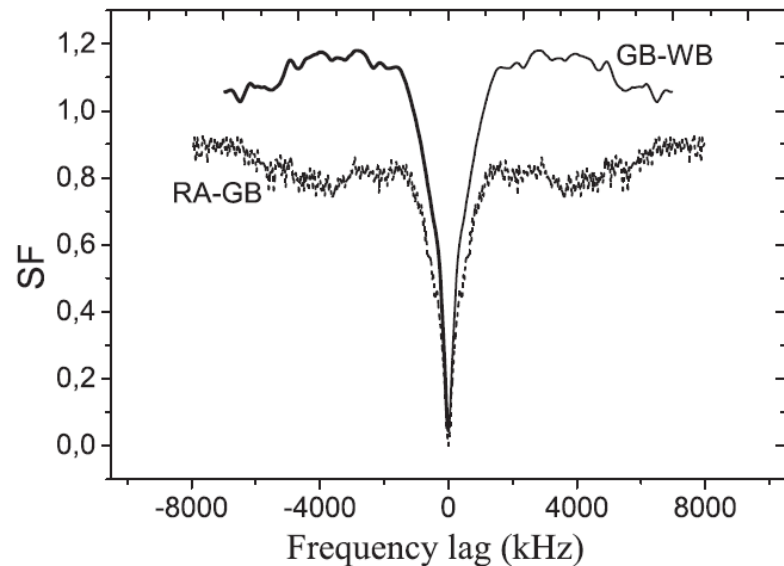
$$\frac{J_1(\vec{b}_s, \Delta f > \Delta f_{dif})}{J_1(\vec{b}_s, \Delta f = 0)} = \frac{|B_u(\vec{b}_s)|^2}{1 + |B_u(\vec{b}_s)|^2} = 0.17$$

$$|B_u(\vec{b}_s)|^2 = 0.20$$

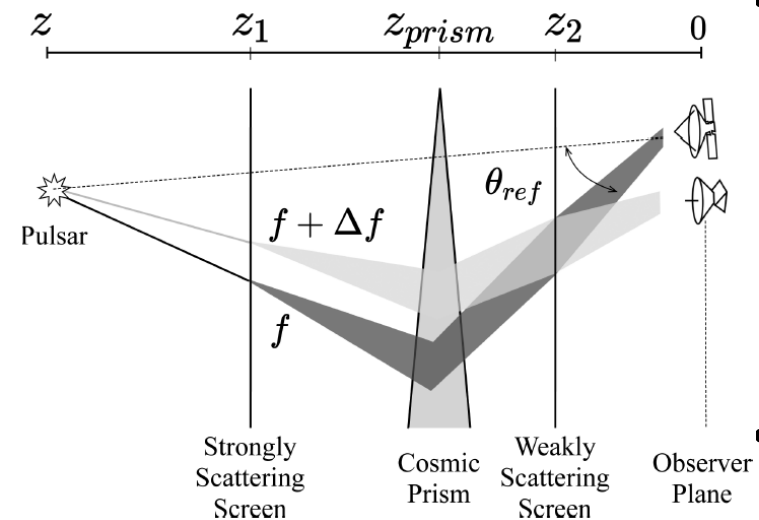
Structure function

$$D_{\Delta I}(\Delta \vec{\rho}) = \langle (\Delta I(\vec{\rho} + \Delta \vec{\rho}) - \Delta I(\vec{\rho}))^2 \rangle_s$$

- Short baseline comprises a narrow-bandwidth component and a broader-bandwidth component.
- The long baseline displays only the narrower frequency-scale component. For the space-ground baseline, a time shift of the structure function produces only a decrease in the amplitude of the structure function, without displacement of its minimum, even with time shifts as large as 800 s. This is consistent with the absence of a wide structure on a long baseline.
- The two frequency scales 0.3 MHz and 2 MHz correspond to two effective layers of turbulent plasma, separated in space, where scattering of pulsar emission take place.
- The shift of SF minimum with increasing time shift is due to refractive shift of the diffraction pattern – the presence of a prism on the line of sight behind the near screen.



ISM structure in direction to PSR B1919+21



- From CCF value on space-ground baseline we can find distance to far screen and scattering angle:

$$b_1 = 6 \times 10^9 \quad |B_u(\vec{b}^*)|^2 = 0.20$$

$$D_s(\vec{b}) = \left(\frac{|\vec{b}|}{\rho} \right)^\alpha, \quad \alpha = n - 2 \quad b_{dif} = \frac{z}{(z - z_1)} \frac{1}{k\theta_{scat,1}} = 4.6 \times 10^9 \text{ cm}$$

$$z_1/(z - z_1) = b_{dif}/(|\vec{V}_p| \Delta t_{dif}) = 0.78$$

$$z_1 = 0.44 z = 440 \text{ pc}$$

$$\theta_{scat,1} = 1.2 \text{ mas}$$

- In observer plane

$$\theta_{obs,1} = [(z - z_1)/z] \theta_{scat,1} = 0.7 \text{ mas}$$

- From the shift of the SF minimum with the maximum time separation, we find the Fresnel scales for the near screen

$$f_{2,0} = 1.1 \text{ M}\Gamma_{\Pi} \Rightarrow t_{2,0} = f_{2,0}(df/dt)^{-1} = 700 \text{ sec.} \Rightarrow \Delta\rho_{2,Fr} = 2^{1/\alpha_2} V_{obs} t_{2,0} = 2.5 \times 10^9 \text{ cm}$$

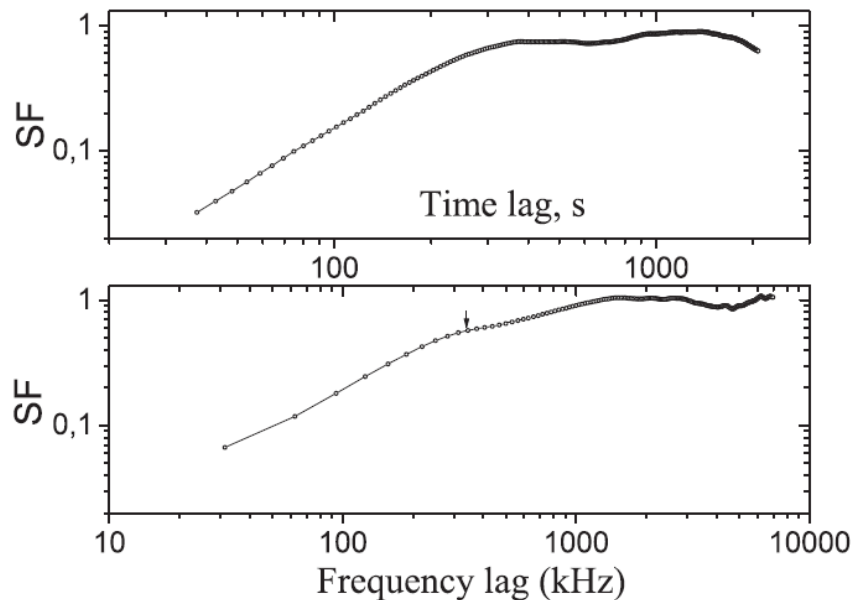
and distance to the screen $\Delta\rho_{2,Fr} = \sqrt{\frac{z_2}{k}} \Rightarrow z_2 = 0.14 \text{ pc}$ $\Delta\vec{\rho}_{2,f} = -2z_2(f/\nu_0)\vec{\theta}_{ref,0} \Rightarrow \theta_{ref,0} = 110 \text{ mas}$

$$D_{S,2}(\Delta\rho_{2,Fr}) = (k\theta_{scat,2}\Delta\rho_{2,Fr})^{\alpha_2} = 0.15 \Rightarrow \theta_{scat,2} = 0.4 \text{ mas}$$

Provided that the refractive displacement is smaller than the scale of the diffraction pattern of scintillations, it is possible to estimate the distance to the prism:

$$2(f_{dif}/\nu_0)z_{prism}\theta_{ref,0} < b_{dif} = 4.6 \times 10^9 \text{ cm} \Rightarrow \begin{cases} f_{dif} = 330 \text{ K}\Gamma_{\Pi} \\ \theta_{ref,0} = 110 \text{ mas} \end{cases} \Rightarrow z_{prism} \leq 2 \text{ pc}$$

Spectrum of density inhomogeneities



- Structure function can be approximated by power-law functions

$$SF(\Delta f) = \frac{1}{2} (\Delta f / \Delta f_{dif})^{\alpha_f} \quad \alpha_f = 0.90 \pm 0.03$$

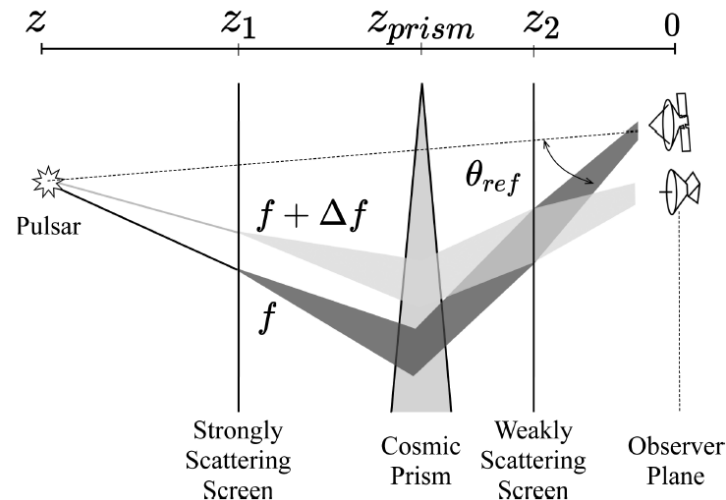
$$SF(\Delta t) = \frac{1}{2} (\Delta t / \Delta t_{dif})^{\alpha_t} \quad \alpha_t = 1.73 \pm 0.02$$

- The power-law index of spectrum of density inhomogeneities

$$n = \alpha_t + 2 = 3.73$$

PSR B1919+21: Main results

- We found for the first time that two scattering regimes are realized in the direction to PSR 1919+21: diffractive scintillations from inhomogeneities in a layer of turbulent plasma at a distance $z_1 = 440$ pc from observer and weak scintillations from a screen located at $z_2 = 0.14$ pc.
- We measured the scattering angles in the direction to PSR B1919+21 as 0.7 mas at 327 MHz.
- We also found that prism with a distance $z < 2$ pc exist in this direction.
- The power-law index of spectrum of density inhomogeneities $n = 3.73$



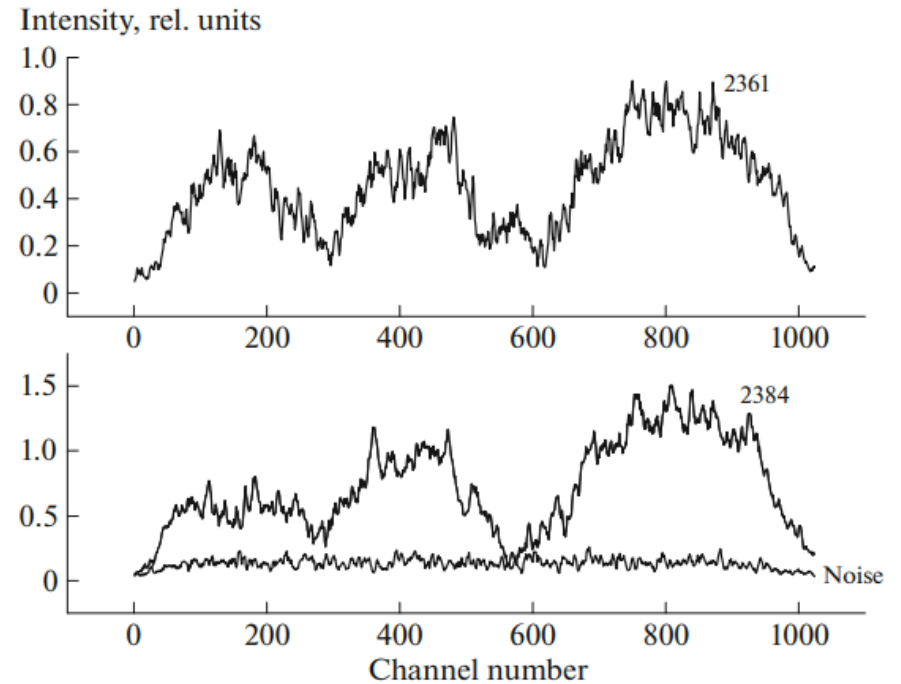
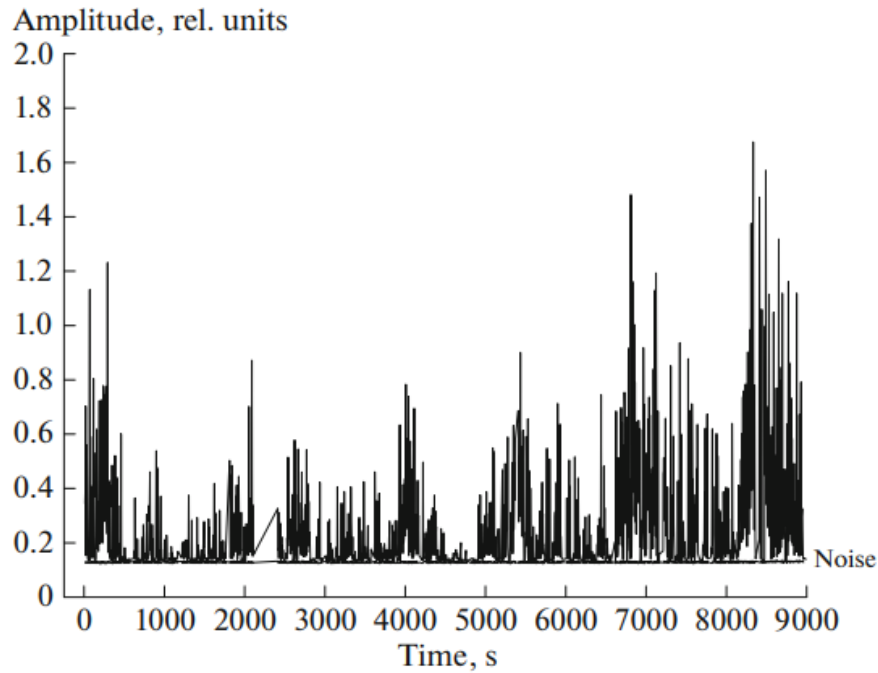
- *Shishov, V. I., Smirnova, T. V., Gwinn, C. R., Andrianov, A. S., Popov, M. V., Rudnitskiy, A. G., & Soglasnov, V. A. MNRAS, 468, 3709 (2017)*

Observations of PSR B0525+21

- 18.09.2013, Projection of base is 233 600 km
- Frequency 1668 MHz, Bandwidth is 16 MHz
- Time duration is 2.5 h
- Telescopes: RA, Green Bank, Arecibo, Kaliazin
- $DM = 50.9$, $Z = 1.6$ kpc, $P_1 = 3.75$ s, ($b = -6.9^\circ$, $l = 183.86^\circ$)

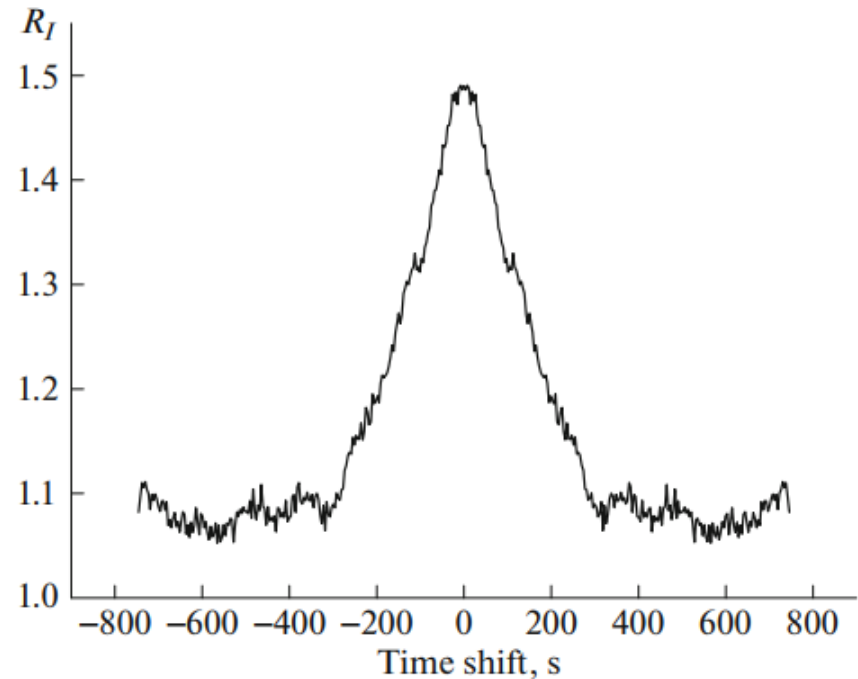
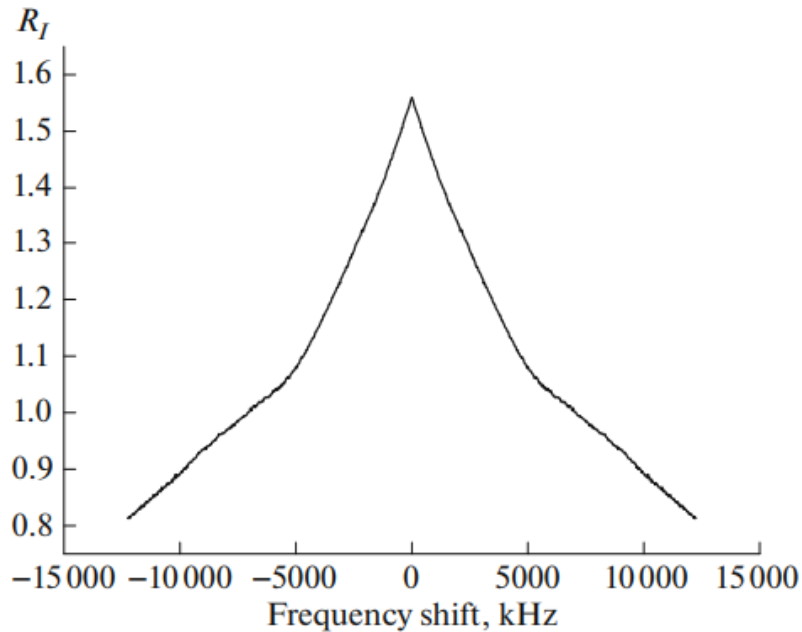
- Correlator ASC FIAN for getting complex cross-spectra.
- On-pulse window includes intensities inside of mean profile on its 0.1 amplitude level (37.45 ms). The off-pulse window was offset from the pulse by half of period.
- Time resolution $\Delta t = 3.75$ s $\Delta f = 15.625$ kHz (1024 channels)

PSR B0525+21



- Modulation index $m = 0.8 \pm 0.2$
- Strong scintillations

Typical scintillation scales



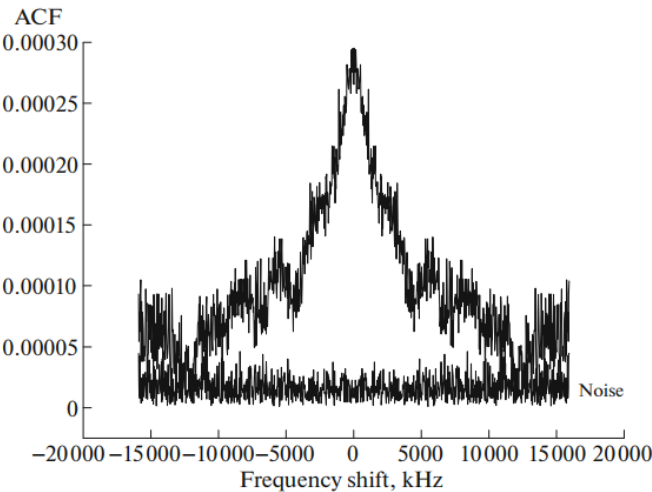
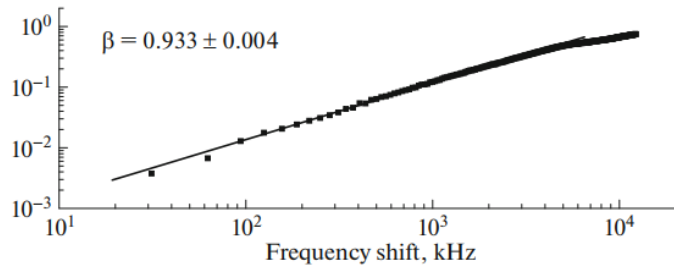
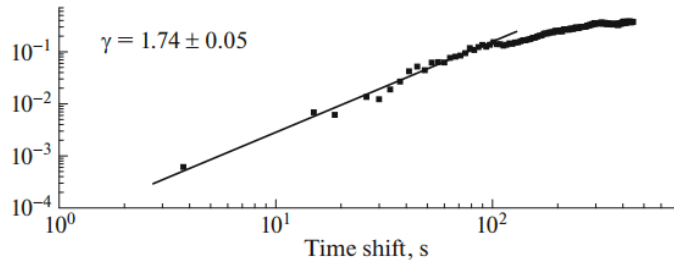
Analysis of mean CCF gives us typical frequency and time scintillation scales

$$\begin{aligned} f_{dif} &= 3.9 \text{ MHz} \\ t_{dif} &= 160 \text{ sec} \end{aligned}$$

$$R_I(\Delta f) = \left\langle \frac{\langle |I(f,t)| \cdot |I(f + \Delta f)| \rangle_f}{[\langle |I(f,t)| \rangle_f]^2} \right\rangle_t$$

Structure function

Structure function



$$D_s(\Delta t) = R_I(\Delta t = 0) - R_I(\Delta t) \quad D_s(\Delta t) = (\Delta t/t_{dif})^\alpha \quad \Delta t \leq t_{dif}$$

$$D_s(\Delta f) = R_I(\Delta f = 0) - R_I(\Delta f) \quad D_s(\Delta f) = (\Delta f/\Delta f_{dif})^{\alpha/2} \quad \Delta f \leq \Delta f_{dif}$$

- The slope of SF indicates a diffractive scintillations model

$$\alpha_t = 1.74 \quad \alpha_f = 0.93$$

- The power-law index of spectrum of density inhomogeneities

$$n = \alpha + 2 \quad \boxed{n = 3.74}$$

- CCF on space-ground baseline

$$J_1(\vec{b}, \Delta f) = |\langle I(\vec{\rho}, \vec{\rho} + \vec{b}, f, t) I^*(\vec{\rho}, \vec{\rho} + \vec{b}, f + \Delta f, t) \rangle|$$

- In the regime of strong scintillation:

$$J_1(\vec{b}, \Delta f) = |\langle j(\vec{\rho}, \vec{\rho} + \vec{b}, f, t) j^*(\vec{\rho}, \vec{\rho} + \vec{b}, f + \Delta f, t) \rangle|$$

$$= |B_u(f)|^2 + |B_u(\vec{b})|^2.$$

$$\frac{J_1(\vec{b}, f > \Delta f_{dif})}{J_1(\vec{b}, \Delta f = 0)} = \frac{|B_u(\vec{b})|^2}{[1 + |B_u(\vec{b})|^2]} = 0.23 \pm 0.05 \Rightarrow \boxed{|B_u(\vec{b})|^2 = 0.30 \pm 0.06}$$

ISM structure in direction to PSR B0525+21

- Spatial Coherence scale

$$\begin{cases}
 B_u(\vec{b}) = \exp[-\frac{1}{2}D_s(\vec{b})] \\
 D_s(\vec{b}) = \left(\frac{|\vec{b}|}{\rho}\right)^\alpha, \alpha = n - 2 \quad \Rightarrow \quad \rho = (2.1 \pm 0.2) \cdot 10^5 \text{ km} \\
 n = 3.74
 \end{cases}$$

- Scattering angle: $\theta_{scat} = 1/k\rho = (0.028 \pm 0.002)$
- The temporal fluctuations of SF are determined by the motion of the

$$D_s(t) = \int_0^Z dz' D\left(\frac{Z-z'}{Z}\vec{V}t\right)$$

- Spatial Coherence scale $\gg Vt_{dif} = 49600 \text{ km}$ The medium is not homogeneous

- We can estimate distance to the screen in thin screen model

$$\Delta f_{dif} = G(\gamma)(kb_s)^2/\pi z_{eff} \quad z_{eff} = z_1(Z - z_1)/Z, \quad b_s = \rho(z_1/Z) \quad G = 0.34$$

$$\frac{z_1/Z}{1 - z_1/Z} = \pi Z \Delta f_{dif} / [G(\gamma)c(k\rho)^2] \quad \left\{ \begin{array}{l} f_{dif} = 3.9 \text{ MHz} \\ \rho = (2.1 \pm 0.2) \cdot 10^5 \text{ km} \\ Z = 1.6 \text{ kpc} \end{array} \right. \Rightarrow \quad z_1/Z = 0.1 \Rightarrow z_1 = 160 \text{ pc}$$

PSR B0525+21: Main results

- Analysis of time and frequency structure functions allowed to conclude that scintillations at 1668 MHz is strong and the diffractive scintillation model is realized.
- The characteristic time and frequency scales of scintillations were determined.
- It is shown that the spectrum of the inhomogeneities of the interstellar plasma is a power spectrum with a power-law index $n = 3.74$.
- The scattering angle in the direction to pulsar PSR B0525 + 21: 0.028 mas.
- We had shown that the scattering of emission from PSR 0525+21 takes place on the screen located close to pulsar: $0.1D$, where D is a distance to pulsar. For $D = 1.6$ kpc we have $z = 1.44$ kpc from the observer.
- *Andrianov, A. S., Smirnova, T. V., Shishov V. I., Gwinn, C. & Popov, M. V. Astronomy Reports, 61, 513 (2017)*

Thank you for attention!

Локальная межзвездная среда



Р. Лалльман, Дж. Линским и Б. Вудом, Спектроскопические исследования

- Локальное межзвездное облако ~ несколько пк
- $T \sim 5-10 \cdot 10^3 \text{ K}$ $n \sim 0.1 \text{ см}^{-3}$
- Локальный пузырь ~ 100 пк
- $T \sim 10^6 \text{ K}$ $n \sim 0.002 \text{ см}^{-3}$

Анализ структурной функции

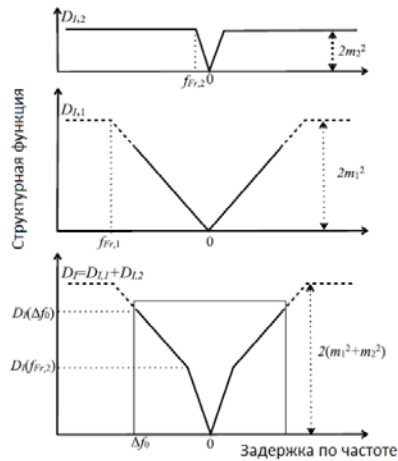


Рисунок 3.5: Схема разделения влияния на структурную функцию эффектов, обусловленных ближним и дальним экранами. Структурная функция для удаленного экрана $D_{I,2}(\Delta f)$ в зависимости от частотного сдвига Δf (верхний график) Структурная функция ближнего экрана $D_{I,1}(\Delta f)$ (средний график). Сумма структурных функций от двух экранов $D_I(\Delta f)$, которой мы моделируем результаты наблюдений на базе Аресибо-Вестерборк (нижний график). Прямоугольник ограничивает область, изображенную на Рис. 3.4. Совместный результат диссертанта и соавторов из работы [A1].

- Структурная функция на короткой базе:

$$D_{I,AR-WB} \equiv D_I = D_{I,1} + D_{I,2}$$

$$D_I(\Delta f) = \begin{cases} 2m_1^2 \left| \frac{\Delta f}{f_{Fr,1}} \right| + 2m_2^2 \left| \frac{\Delta f}{f_{Fr,2}} \right|, & |\Delta f| < f_{Fr,2} \\ 2m_1^2 \left| \frac{\Delta f}{f_{Fr,1}} \right| + 2m_2^2, & f_{Fr,1} > |\Delta f| > f_{Fr,2} \\ m_1^2 + m_2^2, & |\Delta f| > f_{Fr,1} \end{cases}$$

- Наклон меняется $\Delta f = f_{Fr,2} = 3.1 \text{ МГц}$

$$D_I(f_{Fr,2}) \approx 0.5 D_I(\Delta f_0) \quad f_{Fr,2} = 3.1 \text{ МГц и } \Delta f_0 = 8 \text{ МГц}$$

$$\left\{ \begin{array}{l} 2m_1^2 \frac{f_{Fr,2}}{f_{Fr,1}} + 2m_2^2 \approx 0.5 \left(2m_1^2 \frac{\Delta f_0}{f_{Fr,1}} + 2m_2^2 \right) \\ D_I(\Delta f_0) = 2m_1^2 \frac{\Delta f_0}{f_{Fr,1}} + 2m_2^2 \approx 2m^2 \end{array} \right. \Rightarrow \left\{ \begin{array}{l} m_1 = \sqrt{\frac{f_{Fr,1}}{2\Delta f_0 + 2f_{Fr,2}}} m \\ m_2 = \sqrt{\frac{\Delta f_0 - 2f_{Fr,2}}{2\Delta f_0 - 2f_{Fr,2}}} m = 0.15 \end{array} \right.$$

- Используя $f_{Fr,1} > \Delta f_0 = 8 \text{ МГц}$ $f_{Fr,1} < 15 \text{ МГц}$

$$0.32 < m_1 < 0.43$$

- экран 1 ближе к наблюдателю т.к. частотный масштаб Френеля у него больше

Структурная функция флуктуаций фазы на экране

$$D_{S,l}(\Delta \vec{x}_l) = (k\Theta_{scat,l} |\Delta \vec{x}_l|)^{\alpha_l}$$

$$\alpha_1 = \alpha_2 = 1$$

$$D_{I,l}(\vec{r}_l) = \begin{cases} m^2 \frac{|\vec{r}_l|}{\rho_{Fr,l}}, & |\vec{r}_l| < \rho_{Fr,l} \\ m^2, & |\vec{r}_l| \geq \rho_{Fr,l} \end{cases}$$

$$\frac{|\vec{r}_l|}{\rho_{Fr,l}} = \left| \frac{\Delta \vec{\rho}}{\rho_{Fr,l}} + \frac{\Delta t}{t_{Fr,l}} + \frac{\theta_0 \Delta f}{f_{Fr,l}} \right|$$

Космическая призма

- Если наблюдатель движется со скоростью перпендикулярной направлению на пульсар, и если экран 1 движется, то пространственное смещение наблюдателя относительно картины мерцаний увеличивается с изменением времени

$$\vec{\rho}_{t,1} = \vec{V}_1 \Delta t = (\vec{V}_{obs} - \vec{V}_{scr,1}) \Delta t$$

- Если смещение наблюдателя параллельно направлению дисперсии космической призмы, то наблюдатель заметит сдвиг картины мерцаний по частоте, как функцию времени
- Для дальнего экрана учитываем сферичность волны:

$$\vec{\rho}_{f,2} = \frac{z z_2}{z - z_2} \vec{\theta}_f = \vec{V}_2 \Delta t = (\vec{V}_{obs} - \frac{z}{z - z_2} \vec{V}_{scr,2} + \frac{z_2}{z - z_2} \vec{V}_{PSR}) \Delta t$$

- Таким образом, задержка во времени эквивалентна изменению местоположения в направлении линейной комбинации векторов $\vec{V}_{obs}, \vec{V}_{scr}, \vec{V}_{PSR}$

Асимметрия структурной функции

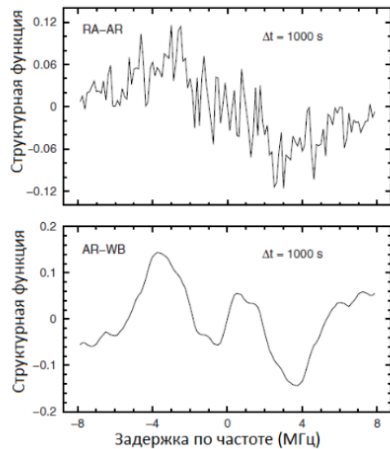


Рисунок 3.7: Отношение разницы структурных функций для положительных и отрицательных частотных сдвигов к их сумме в зависимости от частотного сдвига: для базы РадиоАстрои-Арсибо(верхний график) и Арсибо-Вестерборк(нижний график). Временной сдвиг 1000 сек. Совместный результат диссертанта и соавторов из работы [A1].

- Степень асимметрии:

$$\mathcal{D}(\Delta f, \Delta t) = \frac{D_I(\Delta f, \Delta t) - D_I(-\Delta f, \Delta t)}{D_I(\Delta f, \Delta t) + D_I(-\Delta f, \Delta t)} \quad \Delta f_1 \approx 3 \text{ МГц}$$

- На базе AR-WB два экстремума при $\Delta f > 0$. $\Delta f_2 \approx 1 \text{ МГц}$
- Проекции скоростей экранов имеют разный знак
- На базе RA-AR только минимум при $\Delta f_1 \approx 3 \text{ МГц}$
т.к. RA-AR чувствительна только к ближнему экрану то $\Delta f_1 \approx 3 \text{ МГц}$ связан с экраном 1, а $\Delta f_2 \approx 1 \text{ МГц}$ с экраном 2

- Для базы AR-WB максимум SF: $\left\{ \begin{array}{l} \rho_{Fr,2}/V_2 < \Delta t < \rho_{Fr,1}/V_1 \\ |\Delta \vec{\rho}_{AW}| < \rho_{Fr,2}. \end{array} \right.$

$$\mathcal{D}(\Delta f, \Delta t) \approx \left(\frac{m_2}{m_1} \right)^2 \left(\frac{\rho_{Fr,1}}{\rho_{Fr,2}} \right) \cos \beta_2 \approx 0.05 - 0.1 \cos \beta_2$$

$$\mathcal{D}(\Delta f_2, \Delta t = 10^3 \text{ сек}) \approx 0.05 \rightarrow 0^\circ \leq \beta_2 \leq 60^\circ$$

- Аналогично по минимуму найдем β_1

$$\mathcal{D}(\Delta f, \Delta t) \approx \cos \beta_1 \quad \mathcal{D}(\Delta f_1, \Delta t = 10^3 \text{ сек}) \approx -0.15 \rightarrow \beta_1 \approx 100^\circ$$